J Appl Electrochem (2010) 40:2091–2098
DOI 10.1007/s10800-010-0190-y

ORIGINAL PAPER

An understanding of the electrodeposition process of Al–Mg alloys using an organometallic-based electrolyte

Sankara Sarma V. Tatiparti · Fereshteh Ebrahimi

Received: 26 March 2010 / Accepted: 5 September 2010 / Published online: 18 September 2010

Abstract Al–Mg alloys were deposited using a base-electrolyte with the composition $Na[AlEt_4] + 2Na[Et_3Al–H–AlEt_3] + 2.5AlEt_3 + 6$toluene (where $Et = -C_2H_5$). Mg was introduced into this electrolyte by employing a pure Mg anode. It was found that initially the amount of Mg in the electrolyte increased with the deposition time but eventually a steady state was reached such that the amount of Mg dissolved at the anode became equal to that deposited at the cathode. Compositional and phase analyses indicated that this state is achieved at a critical Mg/Al ratio that resulted in the formation of the hcp Mg-rich phase. By devising various component electrolytes we have attempted to understand the roles of different compounds in the base-electrolyte and have proposed a scheme for the Al–Mg alloy deposition.

Keywords Electrodeposition · Al–Mg alloy · Organometallic electrolyte · Deposition mechanism

1 Introduction

The wide range of properties exhibited by Al–Mg alloys render them suitable for various applications. For example, due to their high volumetric heat content they are used to improve the combustion properties of propellants in aerospace industry [1–5]. Al–Mg alloys also possess excellent corrosion resistance compared to their pure metal counterparts as a result of which they are used as coating materials in automobile industries [6, 7]. Magnesium hydride is an attractive hydrogen storage material [8, 9] and alloying with Al can potentially decrease the dehydrogenation temperature [10], improve the oxidation resistance [11] and increase the heat conductivity [12].

Electrodeposition is a promising technique in producing coatings as well as powders. In the case of Al and Mg, aqueous electrolytes cannot be used for electrodeposition because their reduction potentials (−1.706 V for Al and −2.375 V for Mg) are more negative than the potential for hydrolysis of water. For this reason, Al, Mg and their alloys have been electrodeposited using either molten salts [13–16] or non-aqueous electrolytes [6, 7, 17–21]. For example, using electrolytes consisting of alkali metal fluorides (NaF, KF and CsF), triethylaluminum ($AlEt_3$, where $Et = –C_2H_5$), triisobutylaluminum (iBu_3Al, where $Bu = –C_4H_9$), diethylmagnesium ($MgEt_2$), and toluene as a solvent Mayer could deposit Al–Mg alloys with various compositions [21].

Lehmkuhl et al. [6, 7] developed an electrolyte system for the deposition of Al–Mg alloys with the composition of $Na[AlEt_4] + 2AlEt_3 + 3.3$Toluene. Mg was introduced in the electrolyte by using a pure Mg anode. However, with this electrolyte system they were able to obtain only about a maximum of 24 wt% Mg in the alloys. In order to achieve higher Mg concentration in the deposit, this electrolyte was modified by the addition of another complex component namely, $Na[Et_3Al–H–AlEt_3]$. Although, the addition of $Na[Et_3Al–H–AlEt_3]$ improved the conductivity of the electrolyte, by itself, was shown to have failed in depositing any Mg. However, the reasons for its failure in depositing Mg were not reported in their work. Moreover, Mg anode was shown to develop an unknown dark insoluble layer on its surface during electrodeposition [7]. Also, when the modified electrolyte was used for deposition, the concentration of Mg in the electrolyte was mentioned to

S. S. V. Tatiparti · F. Ebrahimi (✉)
Materials Science and Engineering Department,
University of Florida, Gainesville, FL 32611, USA
e-mail: febra@mse.ufl.edu

build up before reaching a steady state. Again, the reason for this steady state was not clear from their work.

Recently, we have been able to produce Al–Mg alloys with various compositions in the form of powders for hydrogen storage applications using an electrolyte consisting of $Na[AlEt_4]$, $Na[Et_3Al–H–AlEt_3]$ and $AlEt_3$ [9, 22–24]. In the present work, this electrolyte will be referred to as the "base-electrolyte". The Mg content of the deposits was found to depend on the composition of the electrolyte, current density and electrolyte temperature [9, 22]. The amount of Mg in the electrolyte was controlled through a process referred to as the "pre-electrodeposition". During this process, a high purity Mg sheet is employed as anode and the deposition parameters (current density and temperature) are chosen such that the amount of Mg dissolved from the anode is higher than the amount of Mg ions deposited at the cathode, resulting in accumulation of Mg ions in the electrolyte. The Mg-impregnated base-electrolyte can then be used for the electrodeposition of Al–Mg alloys, whose compositions depend on the amount of Mg ions accumulated during the pre-electrodeposition process. In order to control the composition of the Al–Mg alloy, we need to understand the mechanism of Mg build up during the pre-electrodeposition process. Therefore, the objective of the present work was to evaluate the different aspects of the pre-electrodeposition process such as compositional variations and efficiency as a function of time in order to develop a mechanistic understanding of the Mg accumulation. Furthermore, by investigating the roles of different components in the base-electrolyte and the changes in the anode, an attempt was made to present a scheme for the electrodeposition of Al–Mg alloys.

2 Experimental procedures

Depositions were conducted using four different electrolytes namely the base-electrolyte [22] with the composition $Na[AlEt_4] + 2Na[Et_3Al–H–AlEt_3] + 2.5AlEt_3 + 6$ toluene and three different electrolytes, here termed as component electrolytes (C.E.). These electrolytes contained some of the components of the base-electrolyte and are listed below:

(i) $AlEt_3 + 3.3$toluene (C.E. (I))
(ii) $Na[AlEt_4] + 2AlEt_3 + 3.3$toluene (C.E. (II))
(iii) $Na[Et_3Al–H–AlEt_3] + 3$toluene (C.E. (III))

The purpose of investigating the component electrolytes was to understand the roles of different compounds during the deposition process using the base-electrolyte. The results of depositions using component electrolytes (I) and (II) shed light on the role of the $Na[AlEt_4]$ compound and the findings from component electrolyte (III) elucidated the possible effect of the $Na[Et_3Al–H–AlEt_3]$ compound. The chemicals used for the electrolyte preparation were $AlEt_3$ (STREM, 93 wt%, impurities are mixtures of tri-n butylaluminum, diethylbutylaluminum, and ethyldibutylaluminum), Na (ACROS), NaH (ACROS) and toluene (FISHER, laboratory grade). $Na[AlEt_4]$ and $Na[Et_3Al–H–AlEt_3]$ were prepared according to the procedures given elsewhere [22]. Since the different chemicals involved in the present work are highly moisture and oxygen sensitive, they were handled in a glove box with Ar atmosphere, maintaining oxygen and moisture levels of 1 and <7 ppm, respectively.

The depositions were conducted using a rotating cylinder cell setup with a 6 mm nominal diameter copper rod (99.999%) rotating at 200 rpm as a cathode. The Cu rod was electropolished outside the glove box using an electrolyte made of 82.5 vol.% ortho-H_3PO_4 and 17.5 vol.% deionized (DI) water. The polished rod was rinsed with DI water and dried prior to transferring into the glove box. Pure Mg (Goodfellow, 99.9%) sheet in the form of an annular ring was used as anode. A PAR 263 potentiostat/galvanostat interfaced with computer was employed for controlling current as well as for data acquisition. All depositions were conducted at a current density of 60 mA cm^{-2} and a temperature of 90 °C. This current density is beyond the diffusion limiting current density value, i.e. limit current, for the present deposition conditions ($\sim$38 mA cm^{-2}) [22, 25].

In order to study the effect of deposition time on the concentration of Mg, both in the deposits and in the base-electrolyte, depositions were conducted for 20, 80 and 120 min. After each deposition using the base-electrolyte, the Mg anode lost its luster by forming an adherent black film on the surface. The depositions using component electrolytes were consistently conducted for 15 min.

After each deposition, the cathode was cleaned immediately for about 10 min by rotating in fresh toluene and this process was repeated for three times. Then the deposit was scraped off the electrode and used for phase analysis using APD XRD 3720 powder diffractometer with Cu K_α radiation. The presence of the elements in deposits was evaluated using energy dispersive spectroscopy (EDS) in JEOL SEM 6400. The bulk compositional analysis of the deposited Al–Mg powders was conducted using ICP-OES at Columbia Analytics, USA. Since it was difficult to analyze the composition of the electrolyte, the ratio of the Mg/Al ions was evaluated indirectly. After each deposition, the electrolyte was completely oxidized with a 10 vol.% isopropyl alcohol + 90 vol.% toluene mixture. The resulting powder was removed from the glove box, washed with toluene and pelletized and sintered at 1200 °C for 3 h. The resulting pellets were polished and the relative amount of Mg and Al were measured using the EPMA JEOL 733 superprobe. The compositional analysis of each

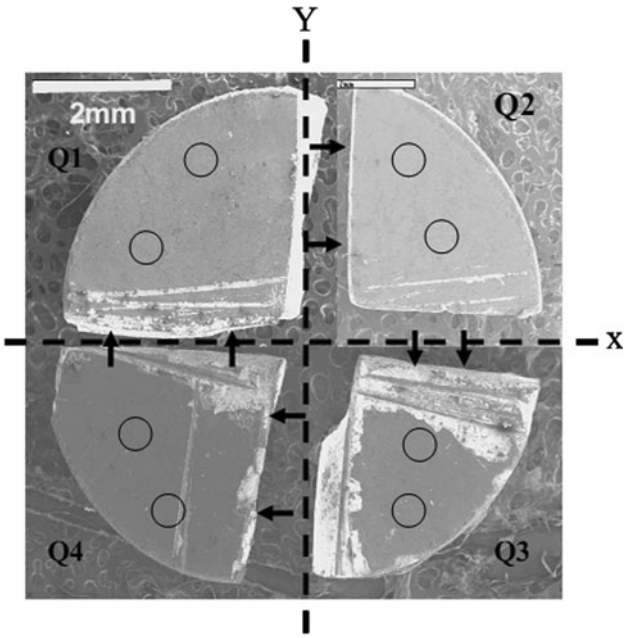

Fig. 1 Low magnification SEM picture of a pellet fabricated from the used base-electrolyte on which compositional analysis was done using the Superprobe. The circles indicate approximate locations where the compositional analysis was performed

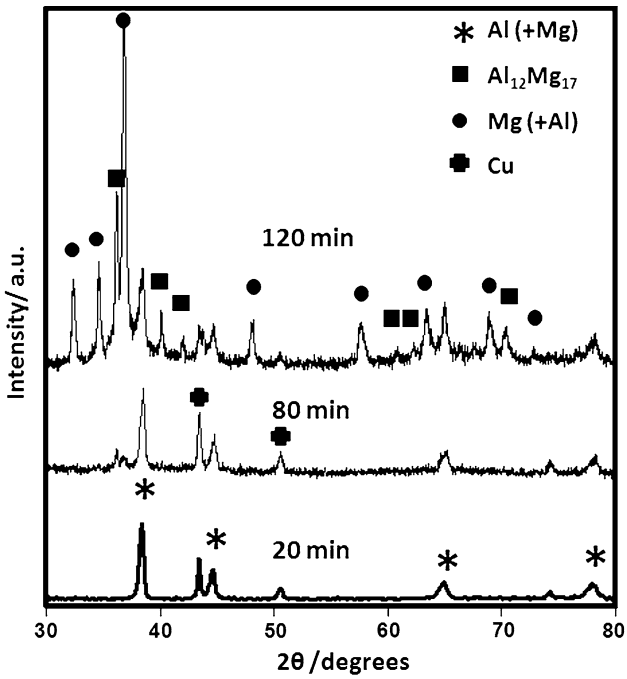

Fig. 2 XRD profiles of deposits prepared using the base-electrolyte after 20 min, 80 min and 120 min at current density of 60 mA cm^{-2} and a temperature of 90 °C

pellet was conducted at many places as shown in Fig. 1. The amount of Mg dissolved in the electrolyte was evaluated by measuring the weight of the anode with an accuracy of ±0.001 g before and after each deposition.

3 Results and discussion

3.1 Phase and compositional analysis

Figure 2 shows the XRD profiles of the deposits prepared for different durations using the base-electrolyte. When the deposition time was 20 min, peaks corresponding to only the face centered cubic (fcc) Al-rich solid solution were observed. After 80 min deposition, in addition to the fcc-Al phase, peaks corresponding to the hexagonal close packed (hcp) Mg-rich solid solution and the intermetallic phase $Al_{12}Mg_{17}$ were found. We have shown previously that under the high deposition rates used here, the formation of the equilibrium intermetallic phases of Al_3Mg_2 and $Al_{12}Mg_{17}$ are inhibited [22]. However, at long deposition times at 90 °C the $Al_{12}Mg_{17}$ phase precipitates within the hcp-Mg phase [9]. Detailed analysis using transmission electron microscopy techniques has revealed that both fcc Al-rich and hcp Mg-rich phases are nanocrystalline and the latter phase always nucleates over the former phase [24]. When the deposition time was increased further to 120 min, the phases remained the same but the relative intensities of the hcp Mg-rich solid solution and the $Al_{12}Mg_{17}$ were increased suggesting an increase in the proportion of the hcp Mg-rich solid solution and $Al_{12}Mg_{17}$ phases. The peaks corresponding to Cu are due to the small amount of Cu that entered into the deposits while scraping them from the electrode.

The average compositions of the deposits as a function of deposition time obtained from ICP-OES analysis are presented in Fig. 3. The results suggest that at lower deposition times (20 and 80 min) the composition of Mg (or Al) increased (or decreased) only insignificantly with the deposition time. However, when the duration of deposition was increased to 120 min, a rapid increase of the Mg (or a decrease of Al) content was observed. The range of deposition times that showed only small changes in the composition of Mg or Al in the deposits is denoted as "stage I" and the range with rapid compositional change is denoted as "stage II" as shown in Fig. 3. Consistent with the low values of Mg contents in stage I, the deposit with 20 min duration showed only the fcc Al-rich solid solution phase. The slight increase in the concentration of Mg in the deposit fabricated for 80 min manifested as the formation of a small amount of the hcp-Mg rich solid solution with some intermetallic $Al_{12}Mg_{17}$ phase. The noticeable increase in the Mg content of the deposit in stage II is correlated with an increased proportion of the hcp-Mg phase. It should be noted that the intermetallic phase forms through a precipitation process in the fcc Al-rich phase and not directly at the deposition front. The longer exposure

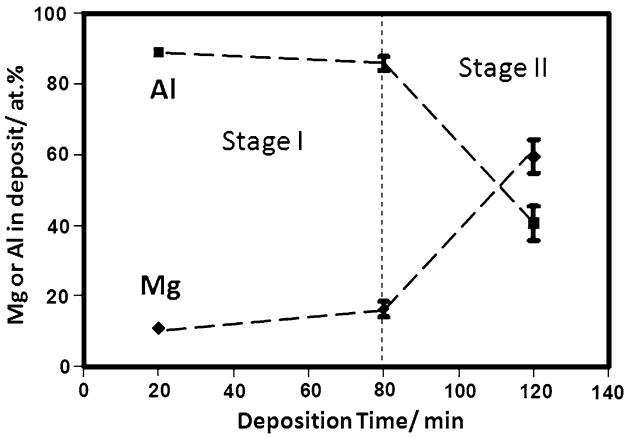

Fig. 3 Compositions of Mg and Al in the deposits as functions of deposition time using the base-electrolyte determined by ICP-OES analysis

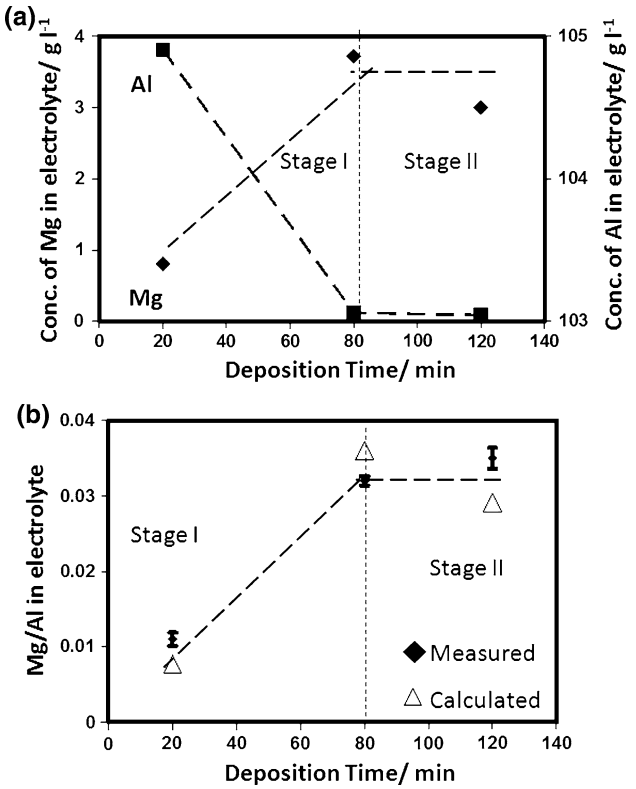

Fig. 4 **a** Calculated concentrations of Mg and Al in the base-electrolyte as function of deposition time. **b** A comparison of experimentally measured Mg/Al concentrations (ICP-OES analysis) with those obtained from the mass balance calculation as a function of deposition time

time has been shown to increase the amount of the precipitate [9].

In order to estimate the concentrations of Mg and Al in the base-electrolyte, different mass balance schemes were adopted for both Mg and Al. In the case of Mg, the anode weight loss was assumed to be equal to the sum of the weight of Mg in the deposit and that accumulated in the electrolyte. In the case of Al, the weight difference between the initially added Al (in the form of different chemical components) and that in the deposit was considered to be left in the electrolyte. The calculated concentrations of Mg and Al in the electrolyte are plotted as a function of the deposition time in Fig. 4a. A comparison of Fig. 3 with Fig. 4a reveals that while the concentration of Mg in deposits does not change considerably during stage I, a sharp increase in the concentration of Mg in the electrolyte takes place with the deposition time in this stage. This observation indicates that there is an accumulation of Mg in the electrolyte during stage I. On the other hand, in stage II, the concentration of Mg in the electrolyte reaches a saturation level (Fig. 4a), whereas the composition of Mg in the deposit increases significantly (Fig. 3). Since the only source of Mg for either the electrolyte or the deposit is through the dissolution of Mg anode, this behavior in the concentration of Mg indicates that most of the Mg dissolved in the electrolyte during stage II enters the deposits, maintaining almost a steady state of Mg concentration in the electrolyte. In order to validate the calculations based on the mass balance, the ratios of Mg/Al measured by analyzing the oxidized electrolytes and those calculated from the above mass balance scheme are compared in Fig. 4b which demonstrates a reasonable correlation. Figure 4b also shows that the Mg/Al ratio increases in stage I and reaches a near constant value in stage II. It is worthwhile to note that the Mg/Al ratio is a small value and its apparent invariability in stage II is a result of constancy of the Mg content.

Figure 5 shows the concentration of Mg in the deposits as a function of the Mg/Al ratio in the base-electrolyte. The curve suggests that a slight change in the Mg/Al ratio in the electrolyte is sufficient to obtain high concentrations of Mg in the deposits. These results indicate that there is a critical condition that needed to be satisfied in order to realize the change in the trends of Mg concentration in the electrolyte (from accumulation to steady state) corresponding to a shift from stage I to II. This critical condition can be correlated with the formation of the hcp-Mg rich solid solution in the deposits. As the Mg/Al ratio at the deposition front increases, proportionally more Mg ions will be reduced at the cathode. Since the solubility of Mg in the fcc-Al phase is limited, the Mg phase will eventually nucleate by the local arrangement of atoms in an hcp crystal structure. Consistently, microstructural observations have confirmed that the hcp-Mg phase always forms over the fcc-Al phase and there is a sharp change in the concentration of Mg across the interface of these two phases [24]. In other words, when the conditions in the deposition front allow the nucleation and growth of the hcp-Mg phase, the rate of

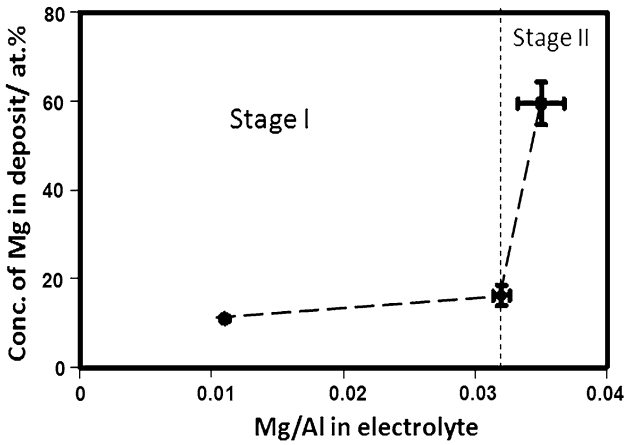

Fig. 5 The concentration of Mg in the deposit as a function of the Mg/Al ratio in the base-electrolyte

Mg ion removal from the electrolyte at the cathode will increase until a steady state is reached. This critical Mg/Al ratio in the electrolyte is expected to be dependent on the experimental conditions such as current density and temperature.

3.2 Roles of different components in the base-electrolyte

Electrodeposition was conducted using the three component electrolytes that were mentioned in Sect. 2 of this paper in order to understand the contribution of the different compounds in the base-electrolyte. When the deposition was attempted with the C.E. (I) electrolyte no deposit was found on the cathode. This observation suggests that $AlEt_3$ is not strongly polar and hence could not be dissociated into ionic species. However, when the C.E. (II) electrolyte was employed for deposition, both Al and Mg were deposited on the Mg anode. Figure 6a shows the EDS spectrum from the deposit indicating the presence of Al and Mg. In this case, contrary to when the base-electrolyte was used, there was no visual change in the luster of the Mg anode. The success of the C.E. (II) electrolyte in depositing Al and Mg may be attributed to the ionic nature of the $Na[AlEt_4]$ compound, which dissociated into Na^+ and $[AlEt_4]^-$ [26].

The deposit from the C.E. (III) resulted in the presence of both Al and Mg as can be seen from Fig. 6b. The presence of Mg in the deposit using the C.E. (III) is in contradiction to the results reported by Lehmkuhl et al., where only Al was found in the deposits [6, 7]. In their studies Lehmkuhl et al. used current density values of about 30 mA cm^{-2} compared to 60 mA cm^{-2} employed in the present study. Decreasing the current density is anticipated to affect both the dissolution rate of Mg at the anode and the relative deposition rate of Mg at the cathode. We

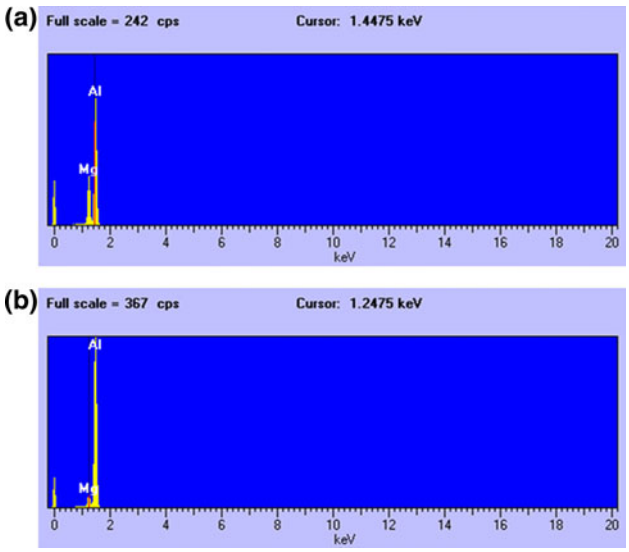

Fig. 6 EDS spectra showing the presence of both Al and Mg in the deposits made from **a** component electrolyte (II) and **b** component electrolyte (III)

have shown previously that the amount of Mg, using the impregnated base-electrolyte, depends on the applied current density as well as the amount of Mg in the electrolyte [22]. Moreover, their anode setup consisted of Al and Mg metals which were connected in parallel, whereas, a pure Mg anode was used in the present study. It was shown elsewhere that employing an anode made of Al and Mg metals would result in a lesser amount of Mg in the deposits compared to when a pure Mg anode was used [9]. Therefore, a low current density and the use of a combination of Al and Mg metals as anodes may reduce the amount of Mg in the electrolyte below the level needed to incorporate detectable amount of it in the deposit.

Similar to when the base-electrolyte was used, a black film was found on the surface of the anode after deposition using the C.E. (III). This film was reasonably adherent on the Mg anode surface. This observation is similar to the studies of Lehmkuhl et al. [7], which reported the appearance of a black insoluble film on the Mg anode. Figure 7 shows the XRD profile of this black film after scraping it from the anode indicating the presence of MgH_2. The peaks corresponding to pure Mg are due to the incorporation of Mg during the scraping of the black film from the Mg anode. The formation of a film has also been observed by other research groups during anodic dissolution of Mg into aqueous electrolytes. In the case of the aqueous electrolytes the black film was identified as MgO [27]. The development of the magnesium hydride film in this study suggests the formation of hydrogen at the anode. The source of hydrogen may be attributed to the dissociation of the $Na[Et_3Al–H–AlEt_3]$ into Na^+ and $[Et_3Al–H–AlEt_3]^-$ and the subsequent breakage of the Al–H–Al

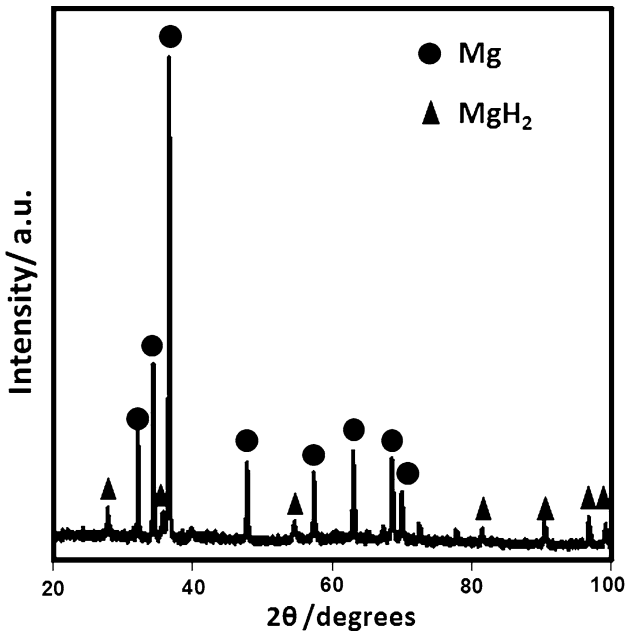

Fig. 7 XRD pattern of the black film found on the Mg anode indicating the formation of MgH_2

bonds to liberate hydrogen according to the following reaction:

$$2[Et_3Al{-}H{-}AlEt_3]^- \rightarrow 4AlEt_3 + 2H_{(ab)} + 2e^- \quad (1)$$

The absorbed hydrogen reacts with Mg to form hydride on the surface of the anode:

$$2H_{(ab)} + Mg \rightarrow MgH_2 \quad (2)$$

When the Al–H–Al bonds are broken, the $AlEt_3$ is released from the complex group and can dissociate further as suggested by Ziegler et al. [26] to result in Al^{+3} as follows:

$$4AlEt_3 \rightarrow 3[AlEt_4]^- + Al^{+3} \quad (3)$$

3.3 Estimation of the Mg valence

In literature, the dissolving Mg ions have been reported as both univalent and divalent when using non-aqueous electrolyte systems [28]. In order to estimate the valence of the dissolving and depositing Mg in the electrodeposition process studied here, the cathodic and anodic reactions were considered. Since it was not possible to quantify the contribution from the reaction involving $[Et_3Al–H–AlEt_3]^-$ complex (Eq. 1) due to the practical difficulties involved in measuring the weight of the black film formed on the surface of the anode, the anodic reaction was assumed to be only the oxidation of Mg. The reductions of Al and Mg were considered as the cathodic reactions. Here, we assumed that the valence of the dissolving and depositing Mg to be the same and denoted as the unknown value (n). The valence of Al was considered to be 3. The assumed anodic and cathodic reactions used for the estimation of the valence of Mg are presented in Eq. 4 and Eqs. 5, 6, respectively. These assumptions are based on 100% efficiency.

Anodic reaction:

$$Mg \rightarrow Mg^{+n} + ne^- \quad (4)$$

Cathodic reactions:

$$Mg^{+n} + ne^- \rightarrow Mg \quad (5)$$

$$Al^{+3} + 3e^- \rightarrow Al \quad (6)$$

Charge balance and mass balance calculations were considered together to estimate the valence of the Mg ion (n). The errors involved from different sources such as equipments (EPMA, weighing balance) were also considered to estimate the variability in the calculated valance values. The estimated valance of Mg as a function of the deposition time is listed in Table 1, which shows that the Mg valence for all the deposition times is nearly close to 2. These values provide an upper bound for the average valence, however, the contribution from the dissociation of the $[Et_3Al–H–AlEt_3]^-$ complex (Eq. 1) is anticipated to be small.

The efficiency values were calculated at different Mg/Al ratios in the electrolyte and are plotted in Fig. 8 by assuming both a valence of 2 for Mg and by considering the estimated values. Since the efficiency values (from both estimated and assumed n) are close any variation in the

Table 1 The estimated valence of the dissolving or depositing Mg ion

Deposition time/min	20	80	120
Valence of Mg (n)	1.9 ± 0.1	1.7 ± 0.1	2.08 ± 0.02

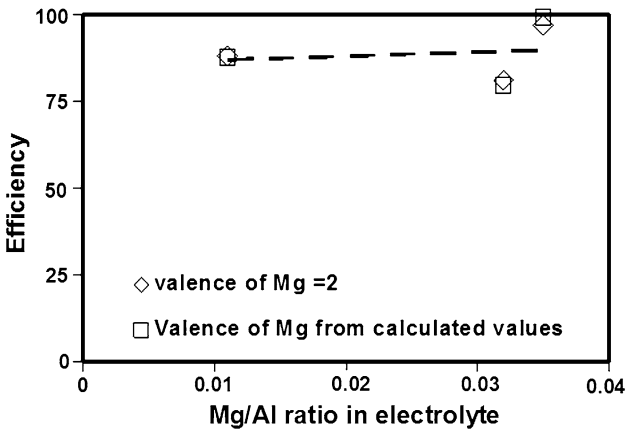

Fig. 8 The efficiency values calculated for deposits made using base-electrolyte with different Mg/Al ratios

efficiency of deposition as a function of the Mg/Al ratio cannot be attributed to a change in the valence of the Mg.

3.4 A scheme for Al–Mg alloy deposition

Considering the observations made in this study and the discussions presented so far, a scheme for the deposition of Al–Mg alloys using the C.E. (III) is proposed as shown in Fig. 9. Aluminum is deposited at the cathode through the reduction of Al^{+3}, which is formed according to Eq. 3. At the same time for each mole of Al^{+3}, a fraction of Mg^{+2}, denoted here as *p/2*, is reduced at the cathode. The anodic reactions consist of the dissolution of magnesium, the dissociation of $[Et_3Al–H–AlEt_3]^-$ (Eq. 1) and the formation of magnesium hydride (Eq. 2). In order to maintain the charge neutrality, for each mole of Al^{+3} reduced at the cathode, (*p/2 + 1/2*) moles of magnesium is oxidized at the anode. For each mole of Al^{+3}, three moles of $[AlEt_4]^-$ (Eq. 3) is generated. One mole the $[AlEt_4]^-$ yields half mole of $Mg[AlEt_4]_2$ and the other two moles of the $[AlEt_4]^-$ is balanced by the two moles of Na^+. The difference between the amount of Mg^{+2} dissolved at the anode, (*p/2 + 1/2*), and the amount of Mg^{+2} reduced at the cathode, *p/2*, explains the accumulation of Mg with the deposition time. It is reasonable to assume that this mechanism operates during stage I (see Fig. 4) using the base-electrolyte. When the composition of the electrolyte is reached to the level that the hcp-Mg phase can form at the cathode, i.e. stage II, the dissociation of $AlEt_3$ is apparently suppressed and most of the Mg^{+2} generated at the anode is deposited at the cathode, thus maintaining a steady state of Mg concentration in the electrolyte (see Fig. 4b).

4 Conclusions

In this study the electrodeposition of Al–Mg alloys using organometallic-based electrolytes consisting of $Na[AlEt_4]$ + $2Na[Et_3Al–H–AlEt_3]$ + $2.5AlEt_3$ + 6toluene (base-electrolyte), $AlEt_3$ + 3.3toluene (C.E. (I)), $Na[AlEt_4]$ + $2AlEt_3$ + 3.3toluene (C.E. (II)), and $Na[Et_3Al–H–AlEt_3]$ + 3toluene (C.E. (III)) was studied. Mg ions were introduced to the electrolyte by using a pure magnesium sheet as anode. Detailed chemical and structural analyses under the conditions used in this study led to the following conclusions:

1. The presence of $Na[AlEt_4]$ is necessary to impart conductivity to the electrolyte.
2. The presence of $Na[Et_3Al–H–AlEt_3]$ leads to the formation of magnesium hydride on the surface of the anode.
3. The deposition takes place in two stages when using the base-electrolyte. In stage I, magnesium is accumulated in the electrolyte. Consequently, the Mg/Al ratio in the electrolyte increases rapidly but the amount of Mg in the deposit increases slightly and only the fcc-Al with Mg as solid solution forms. When the conditions are reached to form the hcp-Mg solid solution (stage II), the Mg/Al ratio as well as their individual concentrations remain almost constant in the electrolyte.

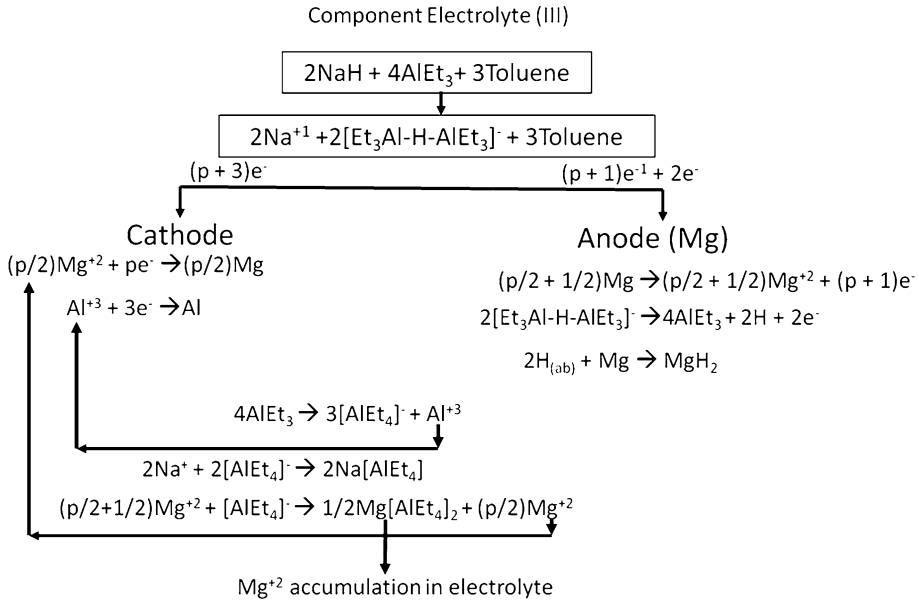

Fig. 9 Al–Mg alloy deposition scheme using component electrolyte (III)

4. The accumulation of Mg during stage I is explained by the formation of the $Mg[AlEt_4]_2$ complex.
5. A small concentration of Mg is sufficient for obtaining high concentrations of Mg in the deposits.

Acknowledgment The support of National Science Foundation under the grant number DMR-0605406 is greatly appreciated.

References

1. Dreizin EL (1996) Combust Flame 105:541
2. Dreizin EL (1999) Combust Flame 116:323
3. Shoshin YL, Mudryy RS, Dreizin EL (2002) Combust Flame 128:259
4. Chen RH, Suryanarayana C, Chaos M (2006) Adv Eng Mater 8:563
5. Dreizin EL, Shoshin YL, Mudryy RS, Hoffman VK (2002) Combust Flame 120:381
6. Lehmkuhl H, Mehler K, Reinhold B, Bongard H, Tesche B (2000) Materwiss Werksttech 31:889
7. Lehmkuhl H, Mehler K, Reinhold B, Bongard H, Tesche B (2001) Adv Eng Mater 3:412
8. Tien HY, Tanniru M, Wu CY, Ebrahimi F (2010) Scripta Mater 62:274
9. Tanniru M, Ebrahimi F (2009) Int J Hydrogen Energy 34:7714
10. Tanniru M (2009) PhD Dissertation, University of Florida
11. Andreasen A, Sorensen MB, Burkarl R, Moller B, Molenbroek AM, Pedersen AS (2005) J Alloys Compd 404:323
12. Zaluska A, Zaluski L, Strom-Olsen JO (2001) Appl Phys A 72:157
13. Carlin RT, Crawford W, Bersch M (1992) J Electrochem Soc 139:2720
14. Zhao Y, VanderNoot TJ (1997) Electrochim Acta 42:1639
15. Jones SD, Blomgren GE (1989) J Electrochem Soc 136:424
16. Borresen B, Haarberg GM, Tunold R (1997) Electrochim Acta 42:1613
17. Legrand L, Tranchant A, Messina R (1994) Electrochim Acta 39:1427
18. Legrand L, Tranchant A, Messina R (1994) J Electrochem Soc 141:378
19. Viestfrid Y, Levi MD, Gofer Y, Aurbach D (2005) J Electroanal Chem 576:183
20. Mayer A (1988) US Patent, 4,778,575
21. Mayer A (1990) J Electrochem Soc 137:2806
22. Tatiparti SSV, Ebrahimi F (2008) J Electrochem Soc 155:D363
23. Tanniru M, Ebrahimi F (2010) Int J Hydrogen Energy 35:3555
24. Tatiparti SSV, Ebrahimi F (2010) J Electrochem Soc 157:E167
25. Tatiparti SSV (2008) PhD Dissertation, University of Florida, USA
26. Ziegler K, Lehmkuhl H (1956) Z Anorg Allg Chem 283:414
27. Greenblatt JH (1956) J Electrochem Soc 103:539
28. Rausch M, McEwen W, Kleinberg J (1955) J Am Chem Soc 77:2093